Electronic Supplementary Information (ESI)

Homochiral coordination polymeric gel: Zn^{2+}-induced Conformational changes leading to J- aggregated helical fibres formation

Mrigendra Dubey, Ashish Kumar and Daya Shankar Pandey*

Department of Chemistry, Faculty of science, Banaras Hindu University, Varanasi- 221005, U.P., India.

E-mail: dspbhu@bhu.ac.in

Table of Contents: **Pages**

Experimental procedures

Materials and Methods: Common reagents and solvents were purchased from Merck, Qualigens or S. D. Fine Chem. Ltd, Mumbai, India and used as received. The solvents were dried and distilled by following standard procedures prior to their use. L-tyrosine, L-leucine, L-phenylalanine were purchased from Sigma Aldrich Chemical Co., USA and used as received.

Elemental analyses for carbon, hydrogen and nitrogen were acquired on an Exeter CHN Analyser CE-440 from the micro analytical laboratory of the Department of Chemistry, Faculty of Science, Banaras Hindu University, Varanasi, India. IR and electronic absorption spectra were obtained on a Perkin-Elmer 577 and Shimadzu UV-1601 spectrophotometers, respectively. ^{1}H spectra were obtained on a JEOL AL 300 FT-NMR spectrometer 300 MHz and Bruker AVANCE III 400. Photoluminescence spectra were acquired on a Perkin Elmer LS 55 spectrophotometer. High resolution mass spectra (HRMS) were obtained on Agilent 6520 Q-Tof mass spectrometer with a capillary voltage of 2.6–3.2 kV. Thermal data were acquired on a Mettler Thermogravimetric Analyzer at a heating rate of 5 °C min^{-1} under a nitrogen atmosphere. Atomic force microscopy (AFM) images were captured using a NT-MDT Solver NEXT Russia. Scanning electron microscopy (SEM) images were captured using a Philips–FEI XL-30 ESEM TMP, Netherland. CD spectra were recorded on a JASCO instrument, Model J-815-150S. Experiments were performed by purging dry N_2 gas continuously at 15 L min^{-1} during data acquisition. Data were collected in a quartz cuvette with a path length of 1 mm between 200 and 400 nm. Rheology of CP gel was performed on Anton Paar Quality Control Rheometer RheolabQC.

Rheological Study: Measurements were performed using a stress-controlled rheometer (Anton Paar Quality Control Rheometer RheolabQC instrument) equipped with stainless steel parallel plates (20 mm diameter, 0.2 mm gap). Experiments were carried out on freshly prepared gels (0.9 %w/v). Linear viscoelastic regions of the samples were determined by measuring the storage modulus, G′ (associated with energy storage), and the loss modulus G″ (associated with the loss of energy) as a function of the stress amplitude. Dynamic oscillatory work was kept at a frequency of 1 rad s^{-1}. The following tests were performed: increasing amplitude of oscillation up to 100% apparent strain on shear, time and frequency sweeps at

20 °C (20 min and from 0.1 to 10 rad s^{-1}, respectively), and a heating run to 100 °C at a scan rate of 1°C min^{-1}. All these measurements were conducted in triplicate.

X-ray Crystallography: Crystals suitable for single crystal X-ray analyses for **6** were directly obtained from the reaction mixture after saturation with acetonitrile. The crystal was mounted on glass fibre. All geometric and intensity data for **6** were collected at room temperature using a Oxford Super Nova CCD diffractometer equipped with a fine focus 1.75 kW sealed tube Mo-Kα (λ = 0.71073 A) X-ray source, with increasing ω (width of 0.3 per frame) at a scan speed of either 3 or 5 s/frame. The strategy for the data collection was evaluated by using the CrysAlisPro CCD software. The data were collected by the standard 'phi-omega' scans techniques and scaled and reduced using CrysAlisPro RED software. Absorption corrections were made using SADABS only as either kinds of absorption did not help.[1] After initial solution and refinement with SHELXL, the final refinements were performed on a WinGX environment using SHELX97.[2a-b] All non-hydrogen atoms were refined anisotropically. Wherever possible, the hydrogen atoms were located from the difference Fourier maps and refined isotropically. Thus, some of the C-H bond will not be ideal and may vary. The asymmetric unit comprises one full copper centre (Cu2), half of a copper centre (Cu1, located on a crystallographic two fold axis), one ligand $H_2T^{L\text{-}leu}$, one acetate ligand and one copper bound axial water molecule (O6) and two water molecules of evacuation of solvent. The application of PLATON-SQUEEZE[2c] command results the removal of prolate ellipsoidal solvent molecule present at four fold axes which leaves the void of 235 $Å^3$ dimension. Because of the prolate ellipsoid of C4 and C5 refinement performed without locating the H atoms on C4 and C5. These atoms are affected by thermal vibrational disorder giving a prolate ellipsoid. There are 24 least-squares restraints used in the refinement to improve the bond length and thermal ellipsoid of isopropyl group as well as lattice solvent molecules. Hydrogen atoms could not be located on Cu(II) bound water molecule (O6) as well as the lattice water molecules (O15 & O16). Thus, the molecular formula and formula weight do not match with crystallographic information file. However, the contribution of missing H atoms are included while experimental data analysis. Selected crystallographic data have been summarized in caption of figure S13.

Theoretical Calculations: Quantum chemical calculations have been performed using a hybrid version of DFT and Hartree- Fock (HF) methods namely the B3LYP,[3] wherein the exchange energy from Becke's exchange functional is combined with exact energy from Hartree-Fock theory. Basis set 6-31G** has been used for C, H, N and O, which combines

quasi-relativistic effective core potentials with a valence double basis-set.[4] The geometry optimization and frequency calculations (to verify a genuine minimum energy structure) were performed using the Gaussian 09 programme.[5]

Synthesis and Characterization:

$H_4T^{-L\text{-}tyr}$(1). L-tyrosine (0.500 g, 2.76 mmol) and $LiOH\cdot H_2O$ (0.173 g, 4.11 mmol) were dissolved in dry methanol (30 mL) and stirred for 30 min at room temperature. Terephthaldehyde (0.185 g, 1.37 mmol) dissolved in the same solvent (10 mL) was added drop wise to the above solution and stirred for an additional 2 hours. Resulting yellow colored reaction mixture was cooled on a ice bath and treated with sodium borohydride (0.419 g, 11.03 mmol) with constant stirring, whereupon the color of solution turned light brown. The brown solution was concentrated to dryness under reduced pressure and ensuing sticky mass was dissolved in water to give a cloudy solution. Upon acidifying with dilute HCl and maintaining the pH between 5-7, it afforded a white solid, which was separated by filteration, thoroughly washed with water, diethylether, and dried under vaccuum. Yield 1.1 g (85%). Anal. Calc. for $C_{26}H_{28}N_2O_6$: C, 67.21; H, 6.07; N, 6.03. Found C, 68.02; H, 6.83; N, 5.79. Due to poor solubility of the neutral form, ^{1}H NMR, ESI-Mass and UV-vis measurements were performed by dissolving the solid in D_2O and methanol in presence of 3 equiv. of $LiOH\cdot H_2O$. ESI–MS (methanol) *m/z*: $[H_4L+H]^+$, 465.2 (calc. 465.2). ^{1}H NMR (400 MHz, D_2O, ppm): δ 7.26 (s, 4H, Ar), 6.94 (d, 4H *J* = 8.4, Ph), 6.54 (d, 4H *J* = 8.4, Ph), 3.72 (d, 2H, $-CH_2Ph$), 3.54 (d, 2H, $-CH_2Ph$), 3.28 (t, 2H, –CHNH), 2.75 (m, 4H, $-CH_2NH$). IR (KBr, cm^{-1}) υ_{as}(COO) 1622(s). UV-vis [methanol, λ_{max}, nm (ε, M^{-1} cm^{-1})]: 280 (2900), 223sh.

$H_4T^{-L\text{-}leu}$(2). This compound was synthesized following the procedure as described for $H_4T^{-L\text{-}tyr}$(**1**) using L-leucine in place of L-tyrosine. Yield 1.3 g (93%). Anal. Calc. for $C_{20}H_{32}N_2O_4$: C, 65.91; H, 8.85; N, 7.69. Found C, 65.99; H, 9.40; N, 7.58. Due to poor solubility of the neutral form, ^{1}H NMR and UV-vis measurements were performed by dissolving the solid in methanol in presence of 2 eqv. of $LiOH\cdot H_2O$. ESI–MS (methanol) *m/z*: $[H_4L+Li]^+$, 371.2 (calc. 371.2). ^{1}H NMR (D_2O, ppm): δ 7.11 (s, 4H, Ar), 3.52 (d, 2H, $-CH_2NH$), 3.32 (d, 2H, $-CH_2NH$), 2.89 (t, 2H, –CHNH), 1.33 (m, 2H, $-CHCH_3$), 1.18 (m, 4H, $-CH_2CH$), 0.64 (dd, 12H, $-CH_3$). IR (KBr, cm^{-1}) υ_{as}(COO) 1573(s). UV-vis [methanol, λ_{max}, nm (ε, M^{-1} cm^{-1})]: 260 (1900).

$H_4T^{-L\text{-}phe}$(3). It was synthesized following the above procedure for $H_4T^{-L\text{-}tyr}$(**1**) using L-phenylalanine instead of L-tyrosine. Yield 1.2 g (92%). Anal. calcd for $C_{26}H_{28}N_2O_4$: C, 72.20; H, 6.53; N, 6.48. Found C, 72.88; H, 7.02; N, 6.37. Due to poor solubility of the neutral form, ^{1}H NMR and UV-vis measurements were performed by dissolving the solid in methanol in presence of 2 eqv. of $LiOH{\cdot}H_2O$. ESI–MS (methanol) *m/z*: $[H_4L+H]^+$, 433.2 (calc. 433.2). ^{1}H NMR (D_2O, ppm): δ 7.07-6.93 (m, 14H, Ar & Ph), 3.46 (d, 2H, $-CH_2Ph$), 3.28 (d, 2H, $-CH_2Ph$), 3.07 (t, 2H, –CHNH), 2.63 (m, 4H, $-CH_2NH$). IR (KBr, cm^{-1}) υ_{as}(COO) 1570(s). UV-vis. [methanol, λ_{max}, nm (ε, M^{-1} cm^{-1})]: 260 (2500).

Coordination polymeric gel (4). A methanolic solution of $Zn(NO_3)_2{\cdot}6H_2O$ (0.060 g, 0.2 mmol) was added drop wise with stirring to a deprotonated solution of the ligand [prepared by treating $H_4T^{-L\text{-}tyr}$ (0.093 g, 0.2 mmol) with KOH, (0.034 g, 0.6 mmol) in MeOH (5 mL) and stirring for 20 min]. The coordination polymeric gel is formed within 2 min upon standing the reaction mixture at room temperature. The resulting gel was dried on rotary evaporator, washed with water to remove impurity of KNO_3 and again dried under vacuum. Yield 0.067g (64%). Anal. Calc. for $[Zn(C_{26}H_{26}N_2O_6)(H_2O)]{\cdot}(CH_3OH)_2$: C, 55.24; H, 5.96; N, 4.60. Found C, 55.36; H, 6.43; N, 4.39. ESI–MS (diluted gel) *m/z*: $[H_3T^{L\text{-}tyr}Zn(CH_3OH)(H_2O)]^+$, 557.1 (calc. 557.1); $[Zn_2(H_2T^{L\text{-}tyr})NO_3(H_2O)].CH_3OH$, 705.9 (calc. 705.3). IR (KBr, cm^{-1}) υ_{as}(COO) 1601(s). Weight loss as per TGA: 13.98 % (calc. for $2CH_3OH$ and H_2O: 14.21 %).

Compound (5). It was synthesized following the above procedure for **4** using $LiOH{\cdot}H_2O$ in place of KOH. It gave a clear solution at room temperature and no gelation was observed even after keeping the solution undisturbed overnight. The resulting solution was dried on rotary evaporator, washed with water to remove impurity of $LiNO_3$ and dried under vacuum. Yield 0.059g (53%). Anal. Calc. for $[Zn(C_{26}H_{26}N_2O_6)(H_2O)]{\cdot}(CH_3OH)_3$: C, 54.36; H, 6.30; N, 4.37 Found C, 54.83; H, 6.74; N, 4.27. IR (KBr, cm^{-1}) υ_{as}(COO) 1613(s).

Compound (6). To a suspension of $H_4T^{-L\text{-}leu}$ (0.100 g, 0.27 mmol) in MeOH (15 mL) a solution of $Cu(OAc)_2{\cdot}H_2O$ (0.052 g, 0.27 mmol) in the same solvent (10 mL) was added dropwise and stirred for 3 hours. The deep blue coloured solution thus obtained was

filtered to remove any solid impurities and filtrate was saturated with acetonitrile and kept undisturbed for crystallization. Rod shaped blue crystals were appeared within 3 days, which were washed with CH_3CN and dried under vacuum. Yield 59%. Anal. Calc. for $[Cu_{1.5}(C_{20}H_{30}N_2O_4)(CH_3COO)H_2O]$: C, 49.47; H, 6.61; N, 5.24. Found C, 49.73; H, 7.43; N, 6.04. ESI–MS *m/z*: $[Cu(H_2T^{L\text{-}leu})(H_2O)_3(CH_3OH)]$ 511.3 (calc. 511.2). IR (KBr, cm^{-1}) υ_{as}(COO) 1603(s). UV-vis. [methanol, λ_{max}, nm (ε, M^{-1} cm^{-1})]: 581 (100), 251 (9400). Weight loss as per TGA: 10.32 % (calc. for 3.5 H_2O: 10.17 %).

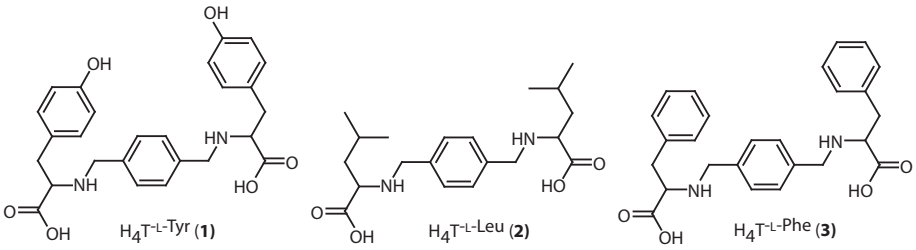

Scheme S1. Structures of **1**-**3**.

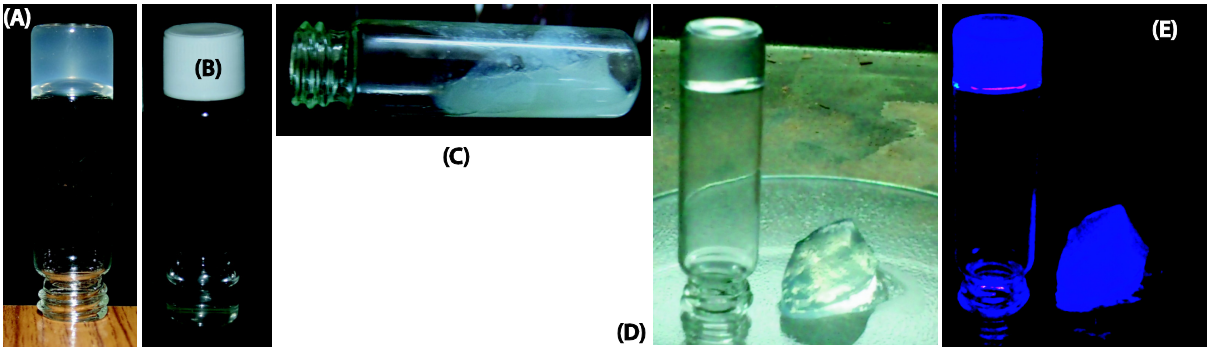

Figure S1. **(A)** CP gel **4** in inverted vial, **(B)** Li^+ containing CP sol **5**, **(C)** Ligand **3** forms gelatinous precipetate in presence of KOH and Zn^{2+} as shown in bent vial, **(D)** CP gel **4** in inverted vial and a cut piece of the gel at room temperature under naked eye in visible light and **(E)** in UV light.

Note: The present CP gel **4** is tight enough that one can cut sharply with desired shape and also can keep for a month in a vial without any change at room temperature.

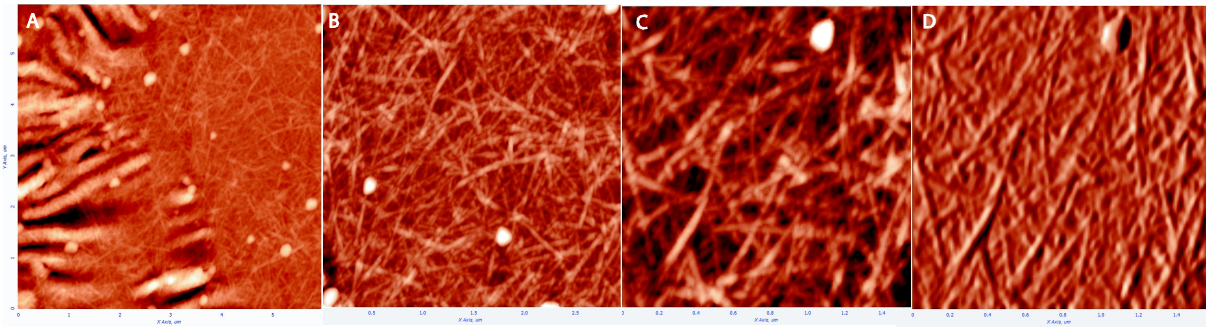

Figure S2. AFM images of CP gel (**A**) fibrous morphology of diluted gel, (**B-C**) magnified from A reveals the twisted fibrous morphology, (**D**) Phase image of C. CP gel was spin-casted on mica before taking the AFM images.

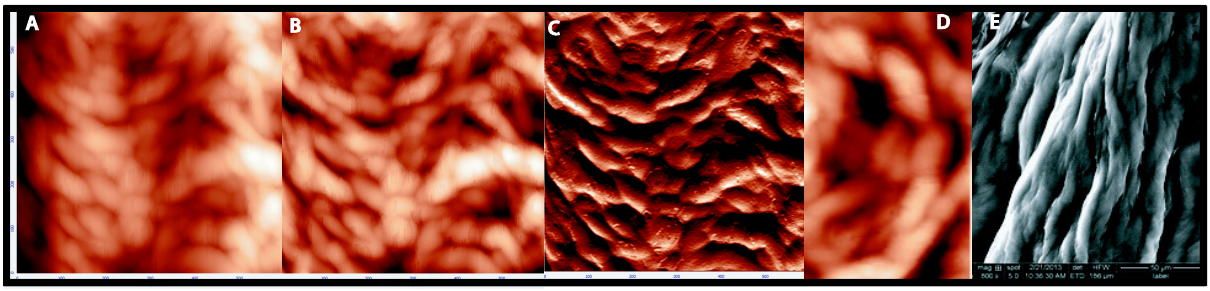

Figure S3. AFM image of CP gel (**A-B**) Twisted fibrous morphology of diluted gel, (**C**) Phase image of B reveals twisted fibrous morphology, (**D**) Magnified image of B showing twisted helical morphology. CP gel was spin-casted on mica before taking the AFM image. (**E**) SEM image of dried CP gel, deposited on silicon wafer before taking the image.

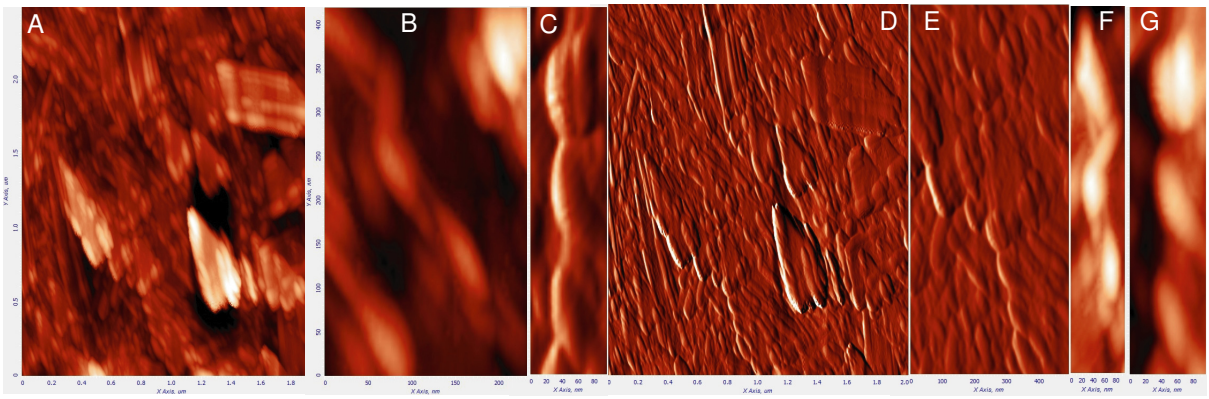

Figure S4. AFM image of CP gel (**A**) Fibrous morphology of diluted gel ($1x10^{-4}$ M), (**B-C**) Magnified image from A reveals twisted helical fibrous morphology, where two fibers are clearly intertwined in helical fashion, (**D**) Phase image of A, (**E**) Cross section of D, (**F-G**) Magnified images of one fiber exhibiting helical arrangement. CP gel was spin-cast on mica before taking the AFM images.

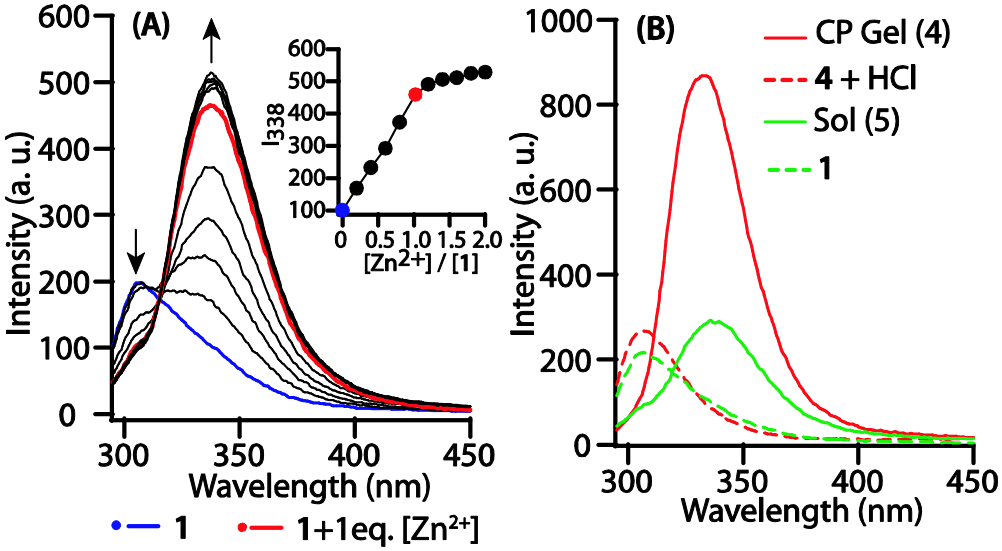

Figure S5. Fluorescence spectra in methanol (λ_{ex} = 280 nm) (A) Titration of 1 (blue) with $Zn(NO_3)_2$ (inset: showing plot between intensity at 338 nm and equiv. of Zn^{2+} added) and (B) CP gel (red continuous line, 0.9% w/v), after treatment with dil. HCl (red dotted line), **1** (green dotted line) and sol **5** (green continuous line).

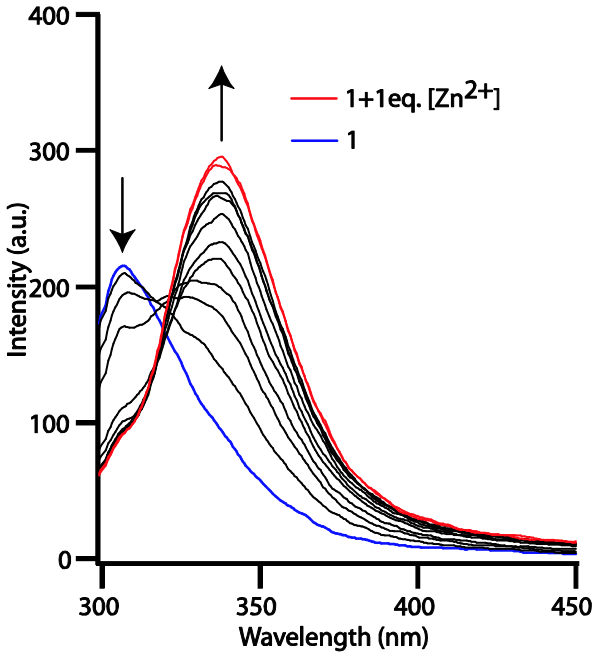

Figure S6. $LiOH.H_2O$ deprotanated **1** ($1x10^{-4}$ M) in methanol (blue line), upon addition of Zn^{2+} gradual decrease in intensity at 306 nm and appearance of a new band at 338 nm, where λ_{ex} = 280 nm. Red lines show saturation after addition of Zn^{2+} (1 equiv.).

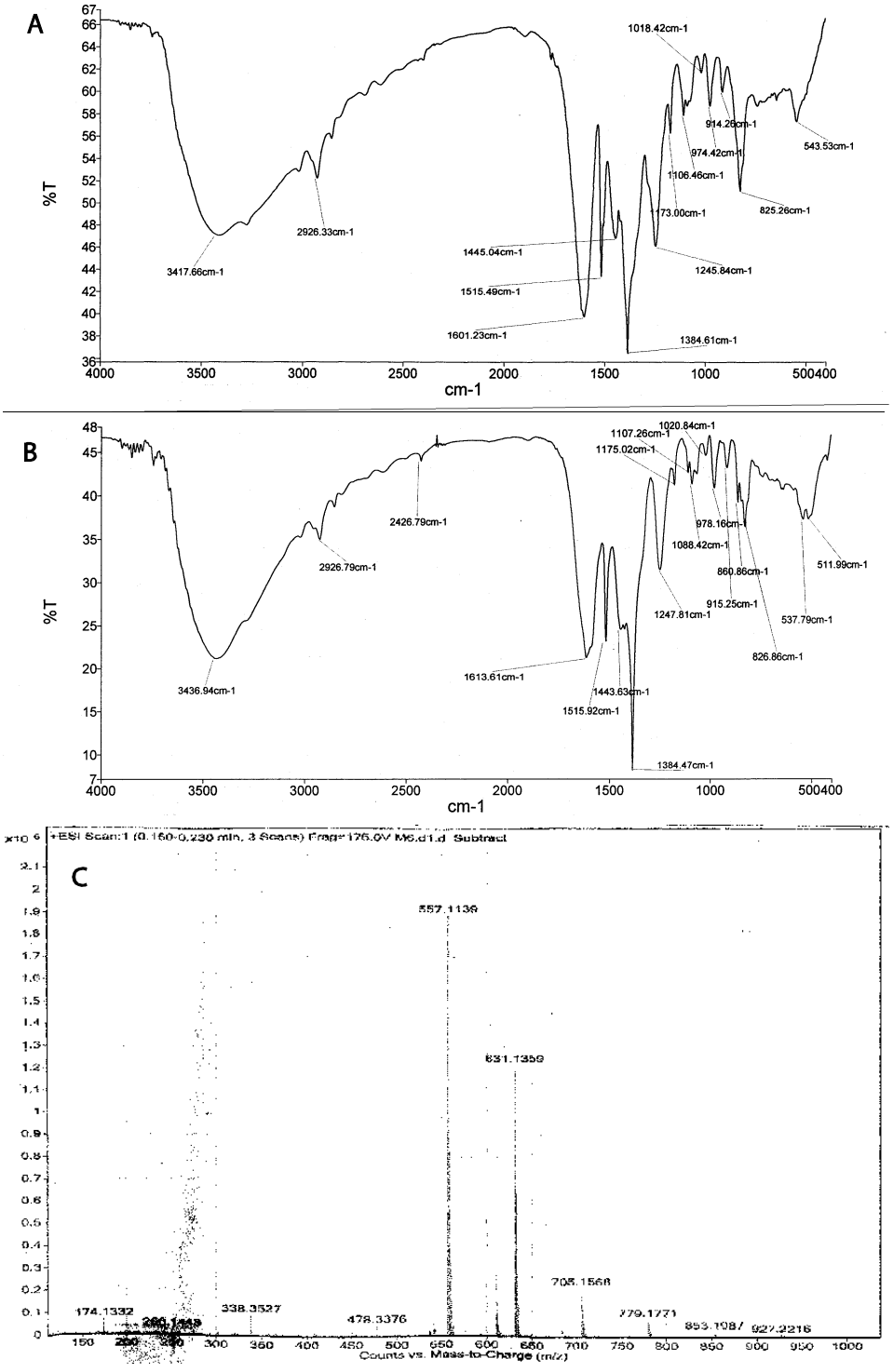

Figure S7. IR spectra of (A) dried CP gel and (B) Li^+ containing dried CP sol. A shift in the $\upsilon(COO)_{asym}$ (~12 cm^{-1}) band clearly indicates the >C=O…Li^+ interaction. Probably the Li^+ interaction interrupts gelation and forms the sol. (C) ESI-MS spectra for CP gel **4**.

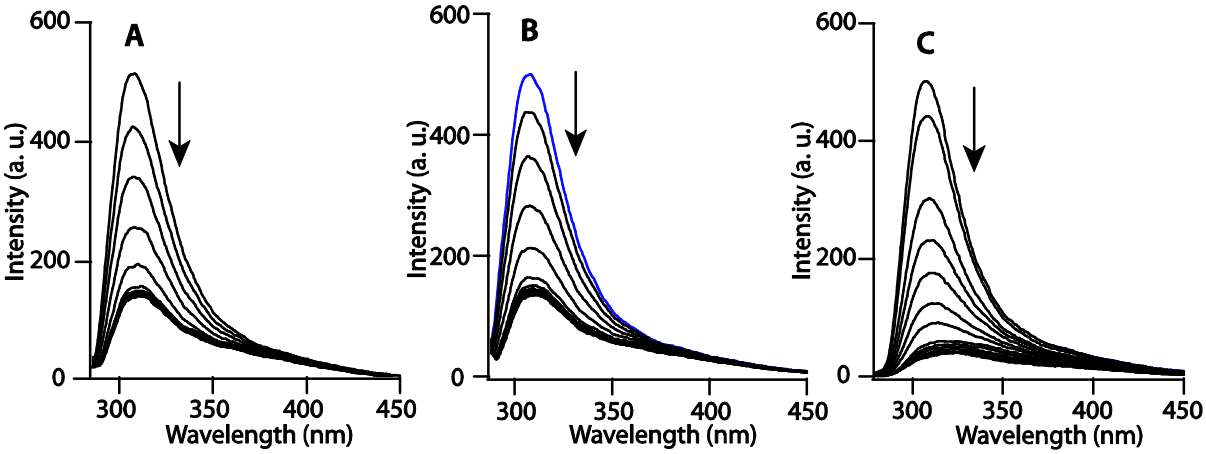

Figure S8. Fluorescence titration of **1** ([**1**] = 2.5x10^{-4} M, deprotonated with KOH) *vs.* **(A)** Co^{2+}, **(B)** Ni^{2+} and **(C)** Cu^{2+} shows quenching at 306 nm (λ_{ex} = 280 nm).

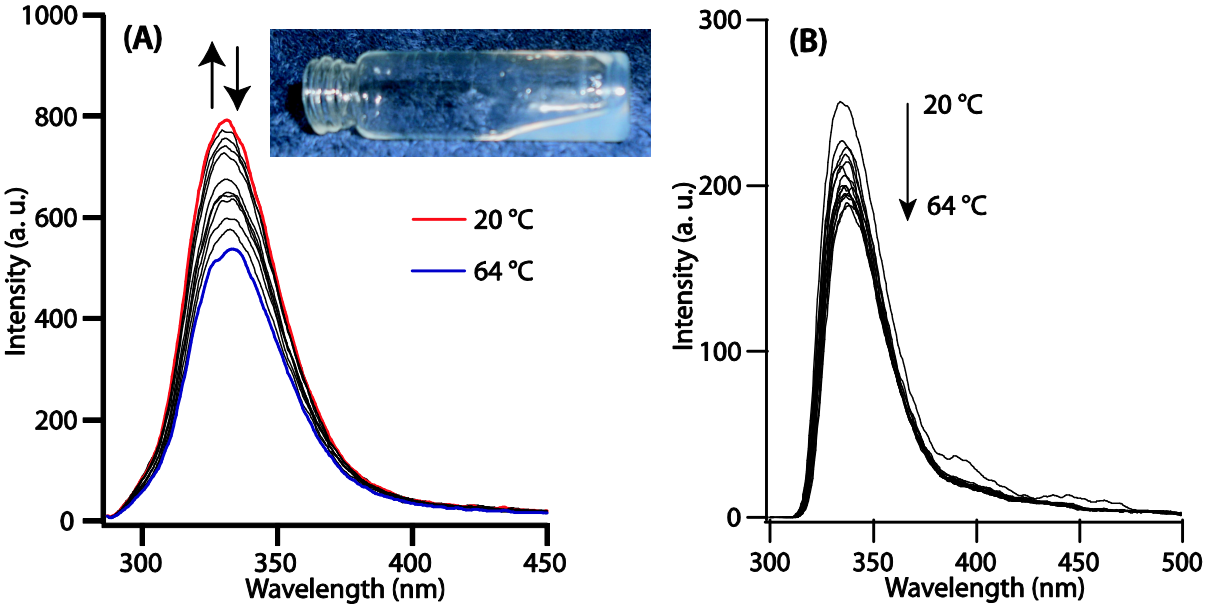

Figure S9. (A) CP gel **4** (0.9% w/v; λ_{ex} = 280 nm at 20 °C) in red line upon heating (4 °C interval) intensity decreases gradualy upto 64 °C (Inset: Viscous gel in vial after heating upto 70 °C). After cooling upto 20 °C, it reversibly gains the initial fluorescence intensity and **(B)** Sol **5** (~ 0.9% w/v; λ_{ex} = 280 nm at 20 °C) upon heating upto 64 °C do not show any significant change as well as after cooling also.

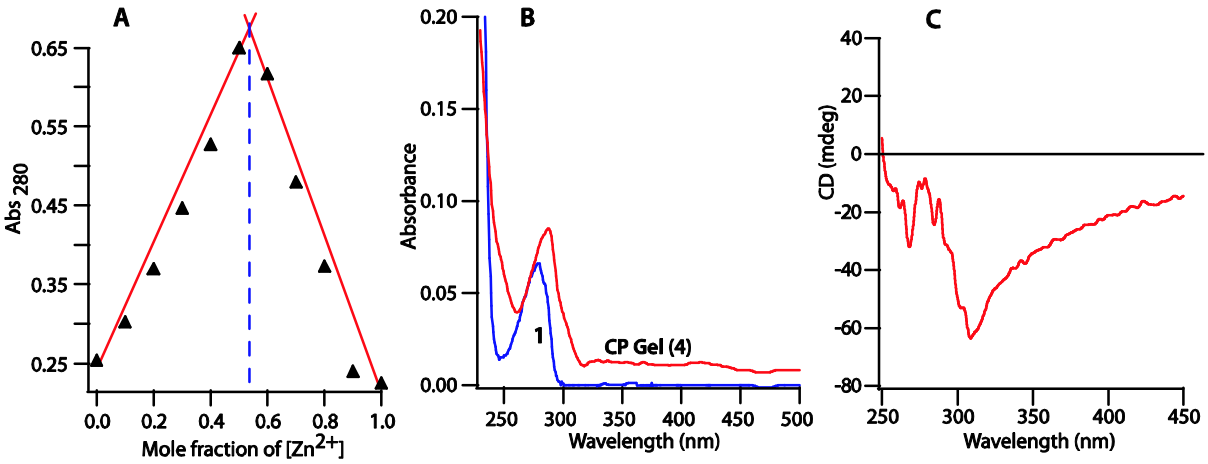

Figure S10. (**A**) Job's plot for **1** with Zn^{2+} showing 1:1 binding ratio performed in methanol, $[Zn^{2+}]/[Zn^{2+}]+[1]$ *vs* absorbance monitored at 280 nm, (**B**) UV-vis spectrum of **1** (deprotonated with KOH, conc. $2x10^{-5}$) in methanol, diluted CP gel (4) in red line exhibits a bathochromic shift ($\Delta\lambda = 12$ nm). (**C**) Solid state CD spectrum of dried CP gel **4** in KBr pellet.

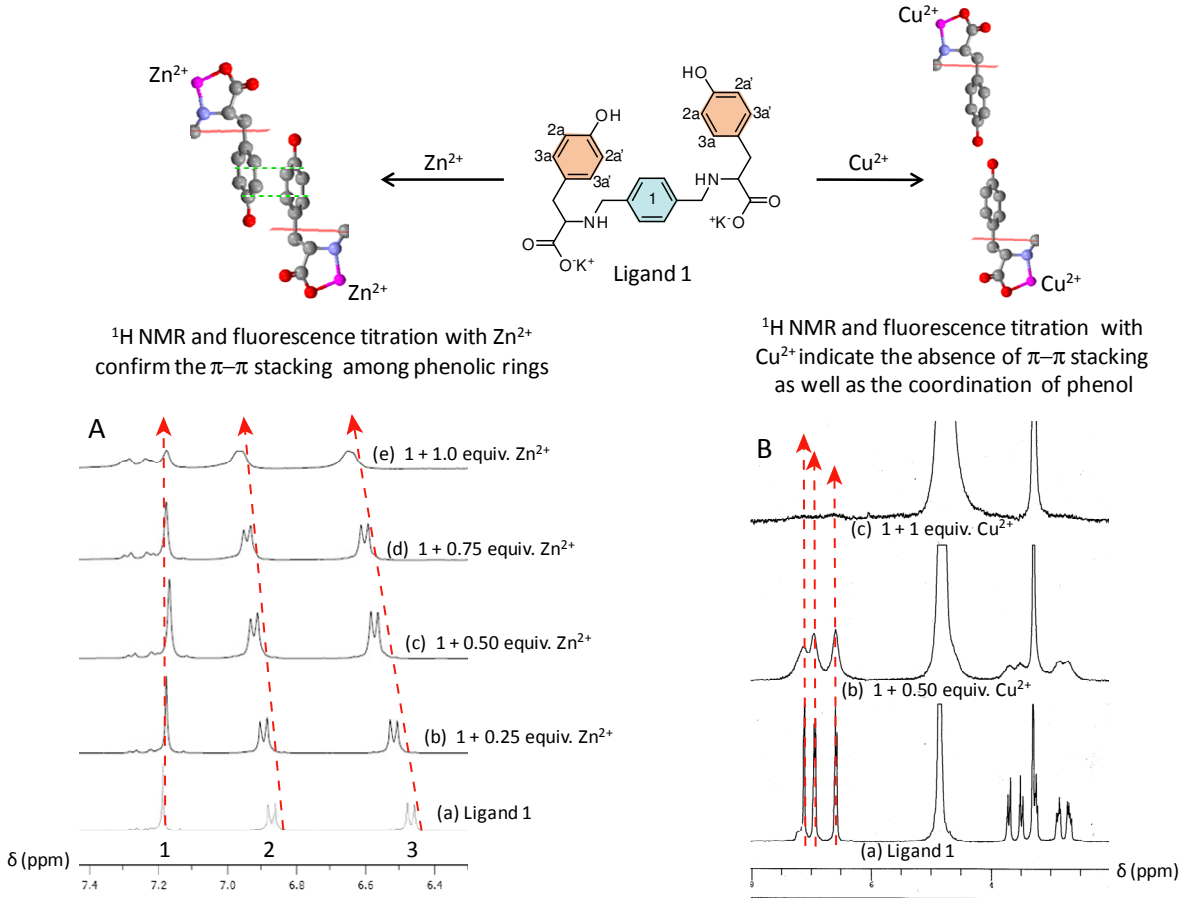

Figure S11. (**A**) ^{1}H NMR titration of **1** (deprotonated with KOH) with $Zn(NO_3)_2.6H_2O$; Aromatic region in the ^{1}H NMR spectra (400 MHz, CD_3OD, 300K) (a) free of Zn^{2+}, with aromatic ring proton resonance appearing at 7.19 (s, 4H, Ar), phenolic ring protons at

6.87 (d, 4H, Ph) and 6.46 (d, 4H, Ph); (b) with 0.25 equivalent of Zn^{2+} added; (c) with 0.50 equivalent of Zn^{2+} added; (d) with 0.75 equivalent of Zn^{2+} added and (e) with 1.00 equivalent of Zn^{2+} added. The spectrum of free ligand, signals associated with the phenolic protons show broadening and significant downfield shift ($\Delta\delta$ = 0.2 and 0.1 ppm) upon addition of Zn2+ (1 equiv.), while no significant changes were observed for other aromatic ring protons (~7.18 ppm), indicates the π–π stacking interactions between phenolic rings. (**B**) ^{1}H NMR spectra of **1** (deprotonated with KOH) titrated with $Cu(NO_3)_2.2.5H_2O$ (400 MHz, CD_3OD, 300K); (a) ligand **1** (b) 0.5 eqv. of Cu^{2+} added, (b) 1.0 eqv. of Cu^{2+} added. There was no significant shift observed after addition of 0.5 eqv. and 1 eqv. of Cu^{2+} except the broadening and disapearance of peaks. The broadening and disapearance for Cu(II) because of the paramagnetic (Cu(II) d9) nature of resultant complex, while broadening of the signals for Zn^{2+} (CP gel) may be because of the additional aggregation (gelation) upon addition of the metal.

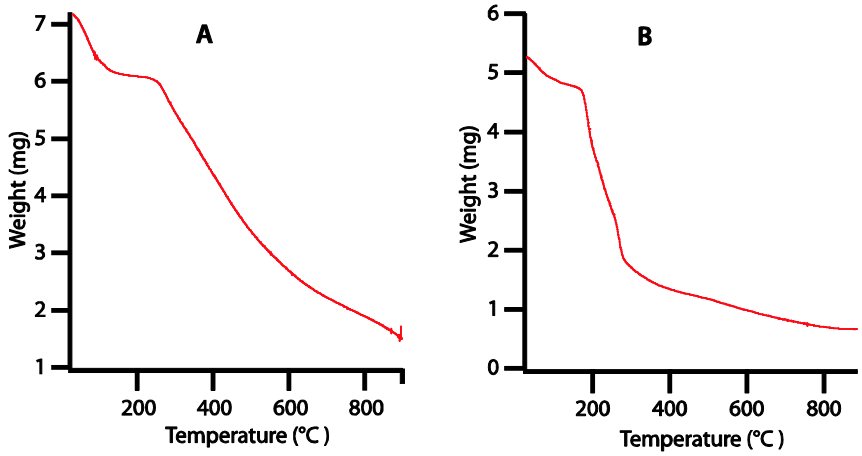

Figure S12. Thermo gravimetric analysis for **(A)** Dried CP gel **4** shows 13.98% weight loss within the temperature range 30–136 °C, which suggests loss of two MeOH and one metal coordinated water molecules, (**B**) CP complex 6 shows 10.32% weght loss over a long temperature range of 30-171 °C, corresponding to the 3.5 H_2O including one coordinated water molecule (2.7% beween range 110-171 °C). Notably, weight loss for one H_2O molecule at higher temperature evidenced coordinated water to metal in CP complex **6** as well as CP gel **4**.

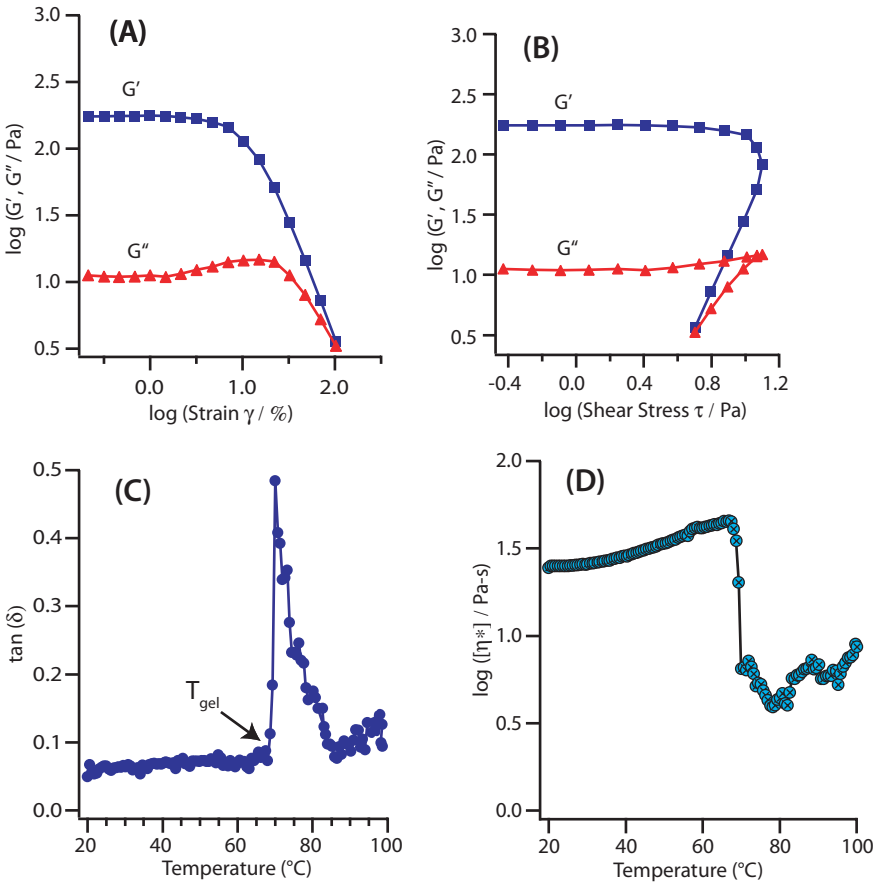

Figure S13. (**A**) Dynamic oscillation strain sweep of G′ and G″ for CP gel **4** at frequency of 1 rad s^{-1} and temperature at 20 °C, (**B**) Dynamic shear stress of G′ and G″ for **4** at frequency of 1 rad s^{-1} and 20 °C, (**C**) Dynamic temperature ramp of loss tangent (tan δ = G”/G’) plot at 1 °C min^{-1}, which indicates the critical temperature (T_{gel}) 67 °C for CP gel and (**D**) Dynamic temperature ramp of complex viscosity measurement at 1 °C min^{-1}.

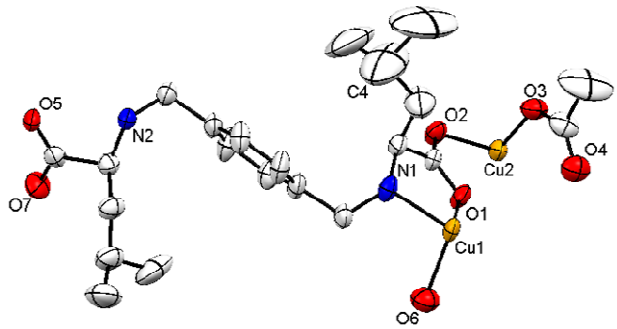

Figure S14. ORTEP diagram of asymmetric unit $[Cu_{1.5}(H_2T^{L\text{-}leu})(CH_3COO)H_2O].2H_2O$ of coordination polymer **6** with thermal ellipsoids set to 40% probability level. Hydrogen atoms and lattice water molecules are omitted for clarity.

Crystal data for 6: Empirical Formula $C_{44}H_{72}Cu_3N_4O_{17}$, Fw 1119.69, T(K) 150(2), tetragonal, '$P42_12$', a = 21.5599(3) Å, b = 21.5599(3) Å, c = 12.8974(3) Å; α = β = γ = 90.00, V = 5995.1(2) $Å^3$, Z = 4, ρ_{calcd} = 1.225 Mgm^{-3}, μ = 1.115 mm^{-1}, reflections

collected 5282, independent 4608, R1 = 0.0476, wR2 = 0.1138 [I > 2σ(I)]; R1 = 0.0570, wR2 = 0.1186 (all data), GOF = 1.052, Flack parameter = -0.011(19). CCDC 962462.

Bond length (Å): Cu1-O1 1.934(3), Cu1-N1 2.047(4), Cu1-O6 2.214(5), Cu2-O5 1.927(3), Cu2-O3 1.942(3), Cu2-N2 2.004(4), Cu2-O2 2.013(3), Cu2-O7 2.233(3).

Bond angle (°): O1-Cu1-O1 169.7(2), O1-Cu1-N1 82.70(14), O1-Cu1-N1 95.25(14), N1-Cu1-N1 157.1(2), O1-Cu1-O6 95.13(10), N1-Cu1-O6 101.45(11), O5-Cu2-O3 176.76(15), O5-Cu2-N2 84.31(14), O3-Cu2-N2 96.92(15), O5-Cu2-O2 89.55(14), O3-Cu2-O2 88.19(15), N2-Cu2-O2 157.44(14), O5-Cu2-O7 96.77(14), O3-Cu2-O7 86.10(14), N2-Cu2-O7 95.51(15), O2-Cu2-O7 106.78(14). H-bond O4…H1A 2.946 Å.

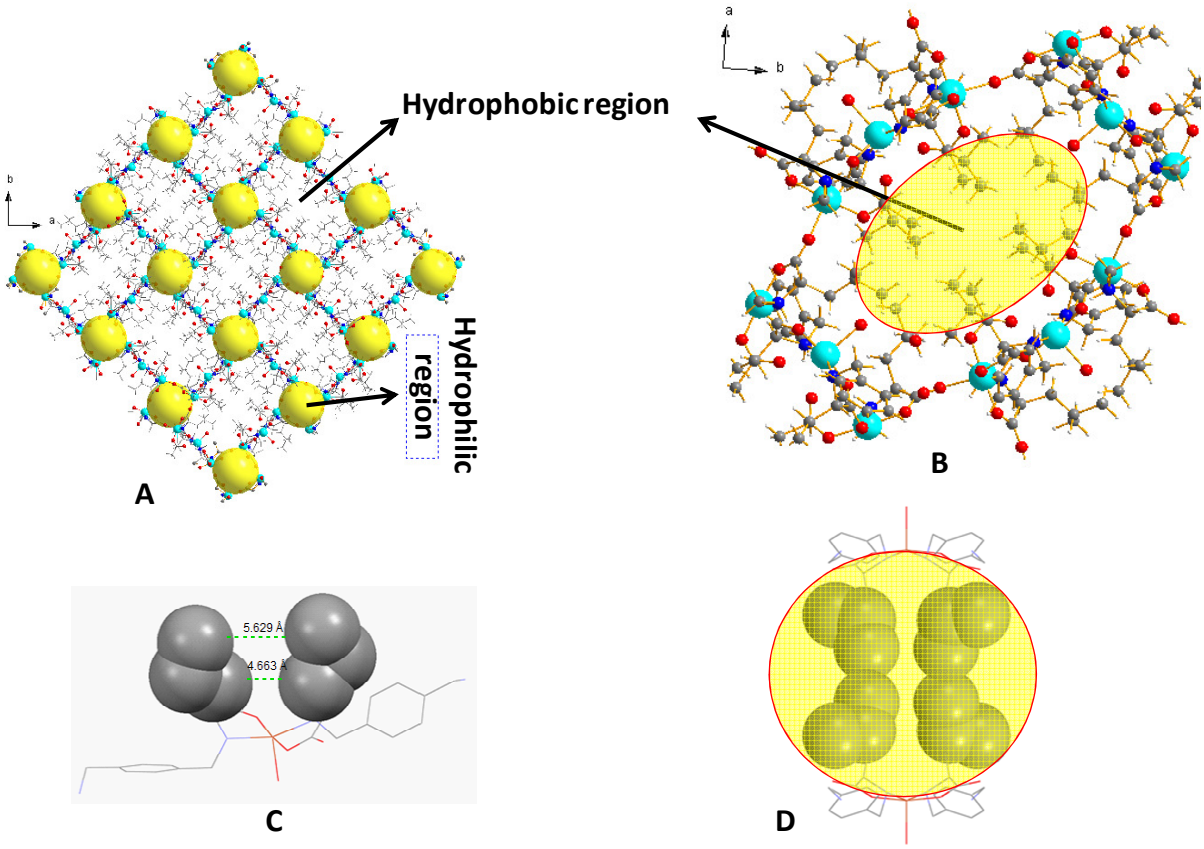

Figure S15. (**A**) Packing of 3D coordination polymer **6** viewed from c-axis showing the hydrophobic and hydrophilic (space filled) pocket separation within the crystal lattice. (**B**) A portion of the A. (**C-D**) Crystal structure of **6** shows the coordination around Cu(II) and the arrangement of hydrophobic L-leucine arm. The π–π stacking is reasonably possible between phenolic rings when replace the L-leucine with L-tyrosine.

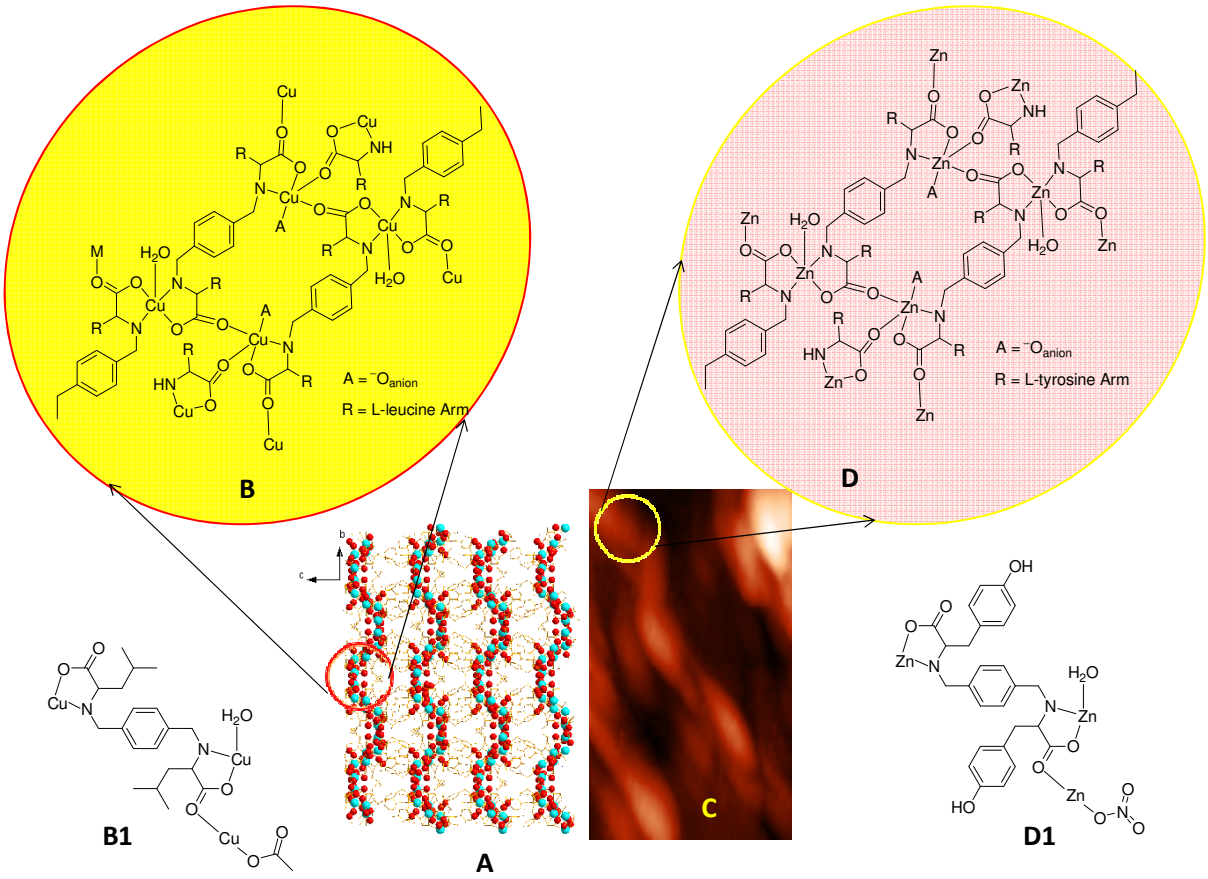

Figure S16. **(A)** Crystal lattice of **6** showing the arrangement of ligand donor atoms around Cu(II) in helical fashion viewed from a-axis, (**B**) A sketch diagram of complex **6** representing the binding mode of ligand with Cu(II) as well as the extension sites for three dimensional coordination polymer in a cross section of lattice, (**B1**) sketch diagram of one unit of **6**. (**C**) AFM image of the CP gel reveals twisted helical fibrous morphology, (**D**) Reasonable sketch diagram of coordination polymer gel 4 represents the ligand arrangement around Zn^{2+} like B, (**D1**) Sketch diagram of one unit of coordination polymer (CP gel 4).

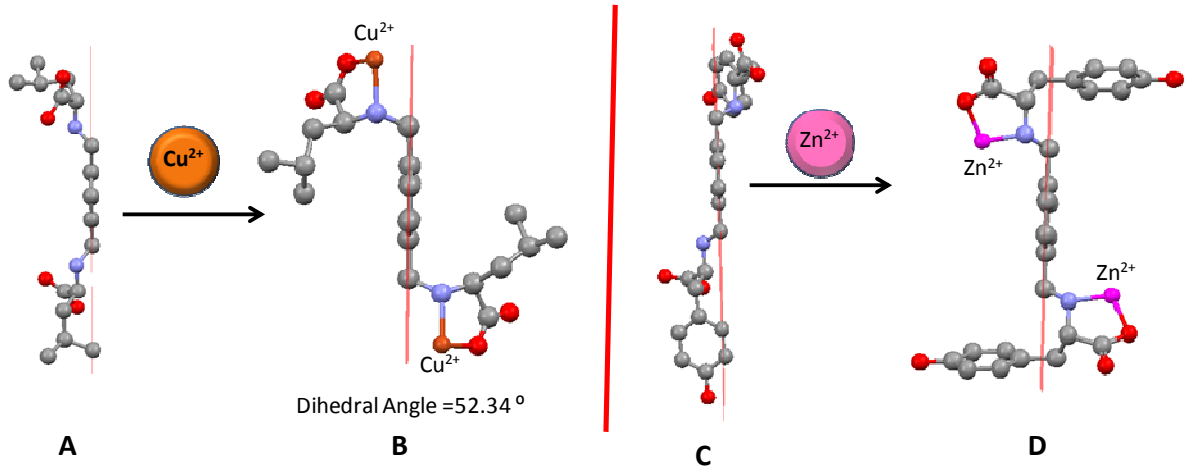

Figure S17. (**A**) The optimized structure of ligand **2** where E = −32432.83 eV, (**B**) Crystal structure of **6** showing the conformational change upon Cu^{2+} coordination with dihedral angle 52.34° considering the metal chelate ring and terephthalic ring, (**C**) Optimized structure of ligand **1** where E = −42682.137855 eV and (**D**) A molecular model of Zn(II) complex on assuming the similar conformational changes like **B** adequately suggests the π–π stacking probability of phenolic rings thereby strongly support the positive response towards gelation.

Note: We could not get the complete optimized structure for CP gel **4** because of overcrowded three dimensional coordination polymeric structure and mentioned above figure (S16 D) is partially optimized structure.

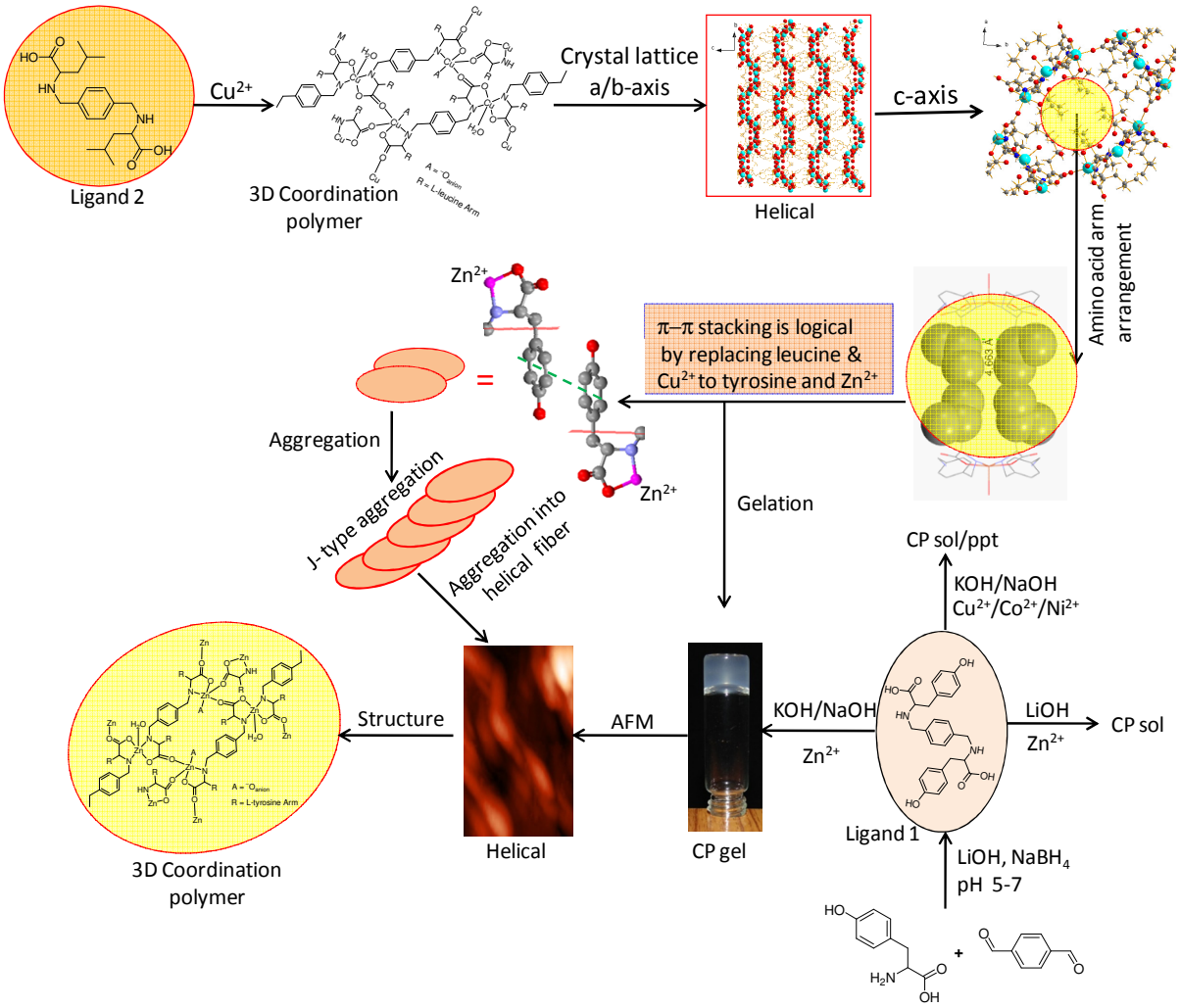

Figure S18. A schematic route for the synthesis of CP gel and CP complex **6** and it's properties as well as the correlation with each other in logical steps; the crystal of the complex **6** solved as three dimentional coordination polymer, perspective view along a or b axis shows the helical arrangement of ligand around Cu(II), while c-axis makes sense about arrangement of hydrophobic leucine arm. Further, the π–π stacking is logical when we substitute L-leucine by L-tyrosine as well as the Cu^{2+} to Zn^{2+}. The π–π stacking is responsible for aggregation which is proved by fluorescence and ^{1}H NMR spectroscopy. J-type aggregation is proved by using fluorescence and UV-vis spectroscopy. Ligand **1** in presence of LiOH and Zn^{2+} forms sol while in presence of KOH/NaOH and Zn^{2+} form CP gel. **1** forms CP sol or precipetate with other metals like Cu^{2+}, Ni^{2+} and Co^{2+}. AFM reveals the twisted helical fibrous morphology. Charaterization of CP gel **4** indicates the strutural similarity with CP **6**.

References:

1 R. Blessing, *Acta Crystallogr., Sect. A* 1995, **51**, 33.

2 (a) G. M. Sheldrick, SHELXL-97: Program for Crystal Structures Refinement; University of Göttingen: Göttingen, Germany, 1997. (b) Farrugia, L. *J. J. Appl. Crystallogr.* 1999, **32**, 837. (c) SQUEEZE option in Platon by P. Sluis, A. L. Spek, *Acta Cryst.* 1990, **A46**, 194.

3 L. J. Bartolottiand, K. Fluchick, *In Reviews in Computational Chemistry*; K. B. Lipkowitz, D. Boyd, Ed. VCH: New York, 1996, **7**, 187.

4 (a) P. Hay, W. R. Wadt, *J. Chem. Phys.*, 1985, **82**, 270; (b) W. R. Wadt, P. Hay, *J. Chem. Phys.*, 1985, **82**, 284; (c) P. Hay, W. R. Wadt, *J. Chem. Phys.*, 1985, **82**, 299.

5 M. J. Frisch, G. W. Trucks, *et al.* Gaussian 09, revision A.1; Gaussian, Inc.: Wallingford, CT, 2009.